Few-Body Syst (2023) 64:72
https://doi.org/10.1007/s00601-023-01839-4

**Sergey Syritsyn · Michael Engelhardt · Jeremy Green ·
Stefan Krieg · John Negele · Andrew Pochinsky**

Nucleon Electromagnetic Form Factors at Large Momentum Transfer from Lattice QCD

Received: 17 April 2023 / Accepted: 13 June 2023 / Published online: 10 August 2023

Abstract Nucleon form factors at large momentum transfer are important for understanding the transition from nonperturbative to perturbative QCD and have been the focus of experiment and phenomenology. We calculate proton and neutron electromagnetic form factors $G_{E,M}(Q^2)$ from first principles using nonperturbative methods of lattice QCD. We have accumulated large Monte Carlo statistics to study form factors up to momentum transfer $Q^2 \lesssim 8\ \mathrm{GeV}^2$ with a range of lattice spacings as well as quark masses that approach the physical point. In this paper, results of initial analyses are presented and compared to experiment, and potential sources of systematic uncertainty are discussed.

1 Introduction

Behavior of nucleon electromagnetic form factors $G_{Ep,n}$, $G_{Mp,n}(Q^2)$ at high momentum transfer $Q^2 \approx 5\dots10\,\mathrm{GeV}^2$ have implications for understanding and improving models of nucleon structure. Models involving vector meson dominance, chiral solitons, a pion cloud, and relativistic constituent quarks have been employed to predict form factor behavior at large Q^2. Generally, while some models may describe data for the four nucleon form factors, their predictions differ in the region where data are unavailable (see, e.g., Ref. [1]

Michael Engelhardt, Jeremy Green, Stefan Krieg, John Negele and Andrew Pochinsky have contributed equally to this work.

S. Syritsyn
Department of Physics and Astronomy, Stony Brook University, Stony Brook, NY 11733, USA
E-mail: sergey.syritsyn@stonybrook.edu

M. Engelhardt
Department of Physics, New Mexico State University, Las Cruces, NM 88003, USA

J. Green
Deutsches Elektronen-Synchrotron DESY, 15738 Zeuthen, Germany

F.Krieg
JARA and IAS, Jülich Supercomputing Centre, Forschungszentrum Jülich, 52425 Jülich, Germany

F.Krieg
Helmholtz-Institut für Strahlen- und Kernphysik, Universität Bonn, 53115 Bonn, Germany

F.Krieg
Center for Advanced Simulation and Analytics (CASA), Forschungszentrum Jülich, 52425 Jülich, Germany

J. Negele · P. Pochinsky
Center for Theoretical Physics, Massachusetts Institute of Technology, Cambridge, MA 02139, USA

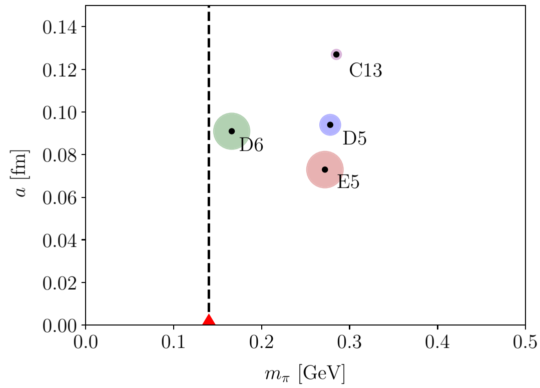

Fig. 1 Lattice ensembles and statistics accumulated for each value of a and m_π. The circle areas are proportional to the number of samples. Lighter pion-mass calculations (D5) require significantly more statistics

for a review). Studies of nucleon form factors using Dyson-Schwinger and Faddeev equations have demonstrated the significance of diquark correlations for the nucleon electromagnetic structure at high momentum transfer [2]. In particular, the zero crossing in the electric Sachs form factors depend on quark correlations in Faddeev's amplitude of the nucleon, thus data from experiment or nonperturbative lattice QCD calculations can be used to determine their magnitude. The experimental program to determine nucleon form factors up to $Q^2 \approx 18\,\text{GeV}^2$ is well underway [3–7], and the first results have been published for the proton magnetic form factor $G_{Mp}(Q^2)$ for Q^2 up to $\approx 16\,\text{GeV}^2$ [8]. This calls for ab-initio theoretical calculations of nucleon form factors with rigorous control of systematic effects, which is possible using modern lattice QCD methods.

Until recently, studies of nucleon form factors on a lattice have been limited by $Q^2 \lesssim 1\ldots2\,\text{GeV}^2$. One notable exception is the calculation of the G_{Ep}/G_{Mp} ratio using Feynman-Hellman method [9]. Lattice calculations involving hadrons with large momentum $|\vec{p}| \gtrsim m_N$ are challenging for several reasons. First, Monte Carlo fluctuations of lattice hadron correlators are governed by the energy of the state [10]. The signal-to-noise ratio for the nucleon is expected to decrease $\propto \exp\big[-(E_N(\vec{p}) - \frac{3}{2}m_\pi)\tau\big]$ with Euclidean time τ, making high-momentum calculations especially "noisy". At the same time, excited states of the nucleon, which are expected to introduce large systematic uncertainties, are less suppressed by Euclidean time evolution $\propto \exp\big[-\Delta E_N(\vec{p})\tau\big]$ as the energy gap $\Delta E(\vec{p}) = E_{N,\text{exc}}(\vec{p}) - E_N(\vec{p})$ shrinks with increasing relativistic nucleon momentum $|\vec{p}|$. Both these challenges are best adressed by choosing the Breit frame on a lattice, so that the initial and final momenta of the nucleon are equal to $|\vec{p}^{(\prime)}| = \frac{1}{2}\sqrt{Q^2}$. For example, momentum transfer $Q_1^2 \approx 10\,\text{GeV}^2$ requires nucleon momentum $p_1 \gtrsim 1.6\,\text{GeV}$, which reduces the energy gap $\Delta E_N(0) \approx 0.5\,\text{GeV}$ to $E_N(p_1) \approx 0.3\,\text{GeV}$. Therefore, very large Monte Carlo statistics combined with rigorous analysis of excited states contaminations become absolutely necessary to obtain credible results.

Such large-statistics calculations have been pursued for a few years, with results previously reported in Refs. [11,12]. These calculations have been performed with $N_f = 2+1$ (light and strange) dynamical quarks with the clover-improved Wilson fermion action with lattice spacing $a \approx 0.09\,\text{fm}$. Two values of the pion masses $m_\pi \approx 280$ and 170 MeV used in the calculations allowed to check for light quark mass dependence of the results. Recently, we have extended our work to a finer lattice spacing $a \approx 0.073$ fm ("E5" ensemble), which is absolutely essential to understand discretization effects, a likely source of systematic errors in calculations involving large momenta. In this paper, we report results obtained on these finer lattices, as well as those from previous coarser lattices but with substantially increased statistics. Our current results rely on multi-state fits to to assess systematic effects from excited states.

2 Methods

We have performed large-statistics calculations on four ensembles of lattice gauge fields. The summary of our accumulated statistics is shown in Fig. 1 and Table 1.

Table 1 Summary of ensembles, kinematics, and statistics

ens	lat	a [fm]	m_π [MeV]	Nconf	stat	$\frac{t_{\text{sep}}}{a}$	$\frac{t_{\text{sep}}^{\max}}{fm}$	$\frac{Q^2_{\max}}{GeV^2}$
C13	$32^3 \times 96$	0.127	285	210	20,160	$6\ldots10$	1.14	8.3
D5	$32^3 \times 64$	0.094	278	1346	86,144	$6\ldots12$	1.13	10.9
D6	$48^3 \times 96$	0.091	166	2040	261,120	$6\ldots12$	1.09	8.0
E5	$48^3 \times 128$	0.073	272	2080	266,240	$7\ldots14$	1.02	8.0

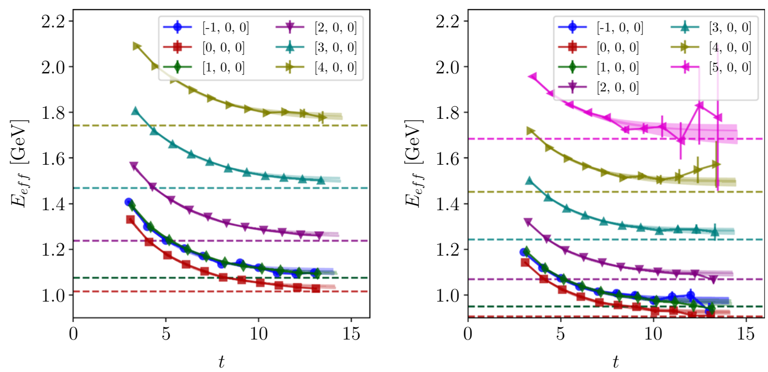

Fig. 2 Nucleon effective energies and ground-state fits computed on ensembles E5 (left) and D6 (right)

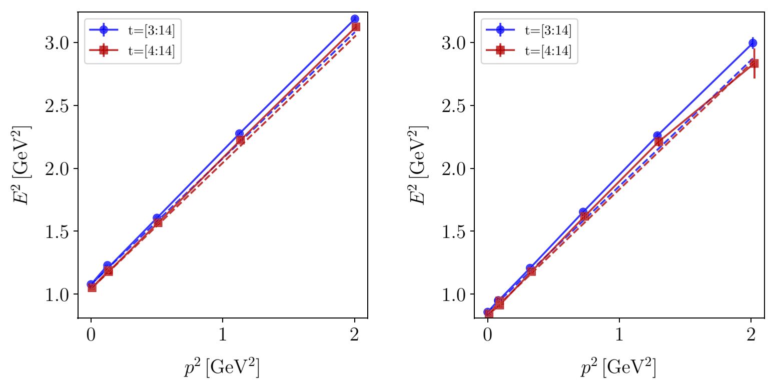

Fig. 3 Dependence of nucleon ground-state energies on momentum computed on ensembles E5 (left) and D6 (right)

In order to obtain nucleon form factors, we calculate nucleon matrix elements of the quark vector current with large-momentum nucleons in the in- and out-states,

$$C_{NV_q^\mu\bar{N}}(\vec{p}', \vec{q}; t_{\text{sep}}, t_{\text{ins}}) = \sum_{\vec{y},\vec{z}} e^{-i\vec{p}'\vec{y}+i\vec{q}\vec{z}} \langle N(\vec{y}, t_{\text{sep}}) [\bar{q}\gamma^\mu q]_{\vec{z},t_{\text{ins}}} N(0)\rangle , \quad (1)$$

where $N = \epsilon^{abc}[\tilde{u}^{aT} C\gamma_5 \tilde{d}^b]\tilde{u}^c$ is the nucleon interpolating field on a lattice constructed with "momentum-smeared" quark fields $\tilde{q}$ to improve their overlap with the ground state of the boosted nucleon [13]. Nucleon matrix elements are extracted from nucleon-current three-point correlation functions using well-established methods of lattice QCD (see, e.g. Ref. [14]). Wick contractions of lattice quark fields generate two types of diagrams: quark-connected and quark-disconnected. The latter have lattice quark "loops" that are connected to the valence quark lines only by the gluons and are more difficult to compute. Their contributions to nucleon form factors at $Q^2 \lesssim 1.2\,\text{GeV}^2$ were found small ($\lesssim 1\%$) [15], but remain to be explored at higher momenta; these contributions are omitted in the current work.

The nucleon correlators become dominated with the ground state $C(t) = \langle N(t)\ldots\bar{N}(0)\rangle \propto e^{-E_N t}$ as the Euclidean time τ is inscreased. As expected, there are substantial contributions from nucleon excited states. Although more than one excited state is expected to contribute, the data are not precise enough to constrain

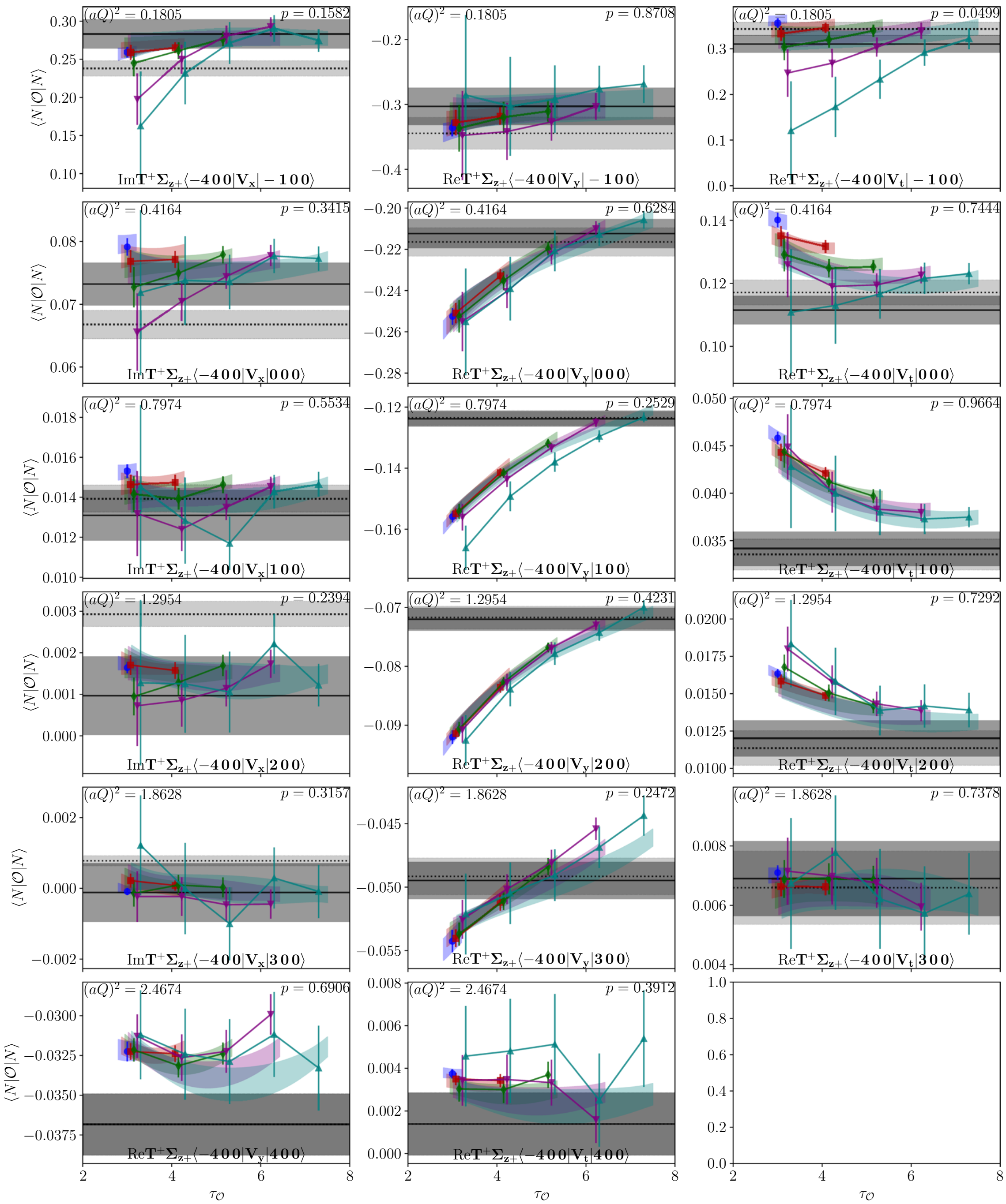

Fig. 4 Fits to the nucleon three-point functions (3) for the D5 ensemble. The colored bands show fits to Eq. (3), the dark-gray bands are the ground-state values $\mathcal{A}_{0'0}$ from these fits, and the light-gray bands are overdetermined fits of these matrix elements to the form factors $F_{1,2}(Q^2)$

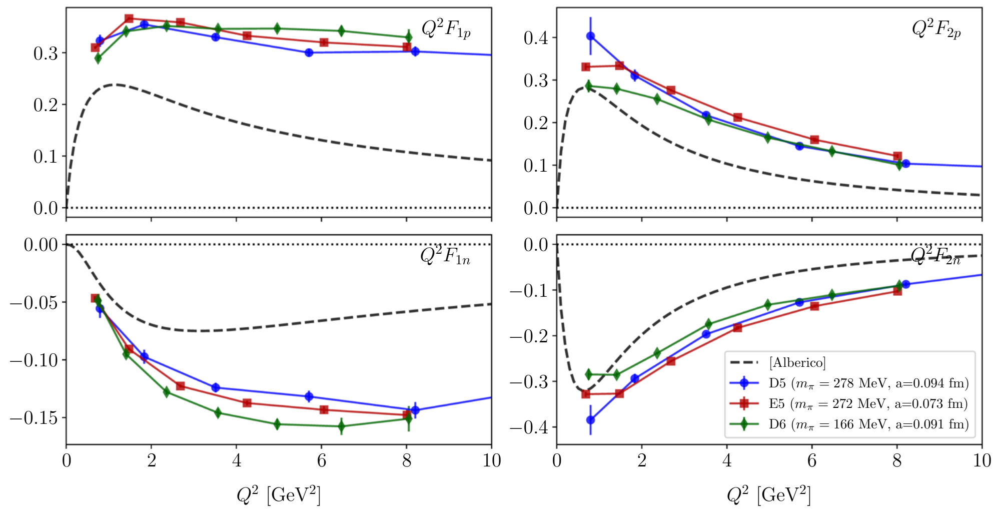

Fig. 5 Comparison of lattice results for Dirac F_1 (left) and Pauli F_2 (right) form factors of the proton (top) and the neutron (bottom) to phenomenological fits of experimental data [16] (dashed curves). Disconnected quark contractions are neglected

more than one, especially at large momenta. Therefore, we impose a simple two-state model on lattice data

$$\langle N(\vec{p},t)\bar{N}(0)\rangle \sim C_0^2 e^{-E_{N0}t} + C_1^2 e^{-E_{N1}t}\,, \tag{2}$$

$$\begin{aligned}\langle N(\vec{p}\,',t)J(\vec{q},\tau)\bar{N}(0) \sim\, & \mathcal{A}_{0'0}C_{0'}C_0 e^{-E'_{N0}(t-\tau)-E_{N0}\tau} + \mathcal{A}_{1'0}C_{1'}C_0 e^{-E'_{N1}(t-\tau)-E_{N0}\tau} \\ & + \mathcal{A}_{0'1}C_{0'}C_1 e^{-E'_{N0}(t-\tau)-E_{N1}\tau} + \mathcal{A}_{1'1}C_{1'}C_1 e^{-E'_{N1}(t-\tau)-E_{N1}\tau}\end{aligned} \tag{3}$$

to extract ground-state nucleon energies $E^{(\prime)}_{N0}$ and momentum-dependent matrix elements of nucleon operators $C_{0^{(\prime)}} = \langle \text{vac}|N|N(\vec{p}^{\,(\prime)})\rangle$ and vector current density $\mathcal{A}_{0'0} = \langle N(\vec{p}\,')|J|N(\vec{p})\rangle$. The fits and the ground-state energies from the former are shown in Fig. 2, together with effective-energy estimators $E_N^{\text{eff}}(t) = \frac{1}{a}\log\left[C(t)/C(t+a)\right]$. The dispersion relation on a lattice $E^2(p^2)$ shown in Fig. 3 indicates that discretization effects in the spectrum of moving nucleons are under control. A representative set of fits of Eq. 3 to three-point *proton* nucleon-current correlator data from the D5 ensemble is shown in Fig. 4. The ground-state matrix elements $\mathcal{A}_{0'0}$ from fits (3) are decomposed into form factors $F^q_{1,2}$ separately for each flavor q. The data points in Fig. 4 show correlator ratios estimating nucleon matrix elements for $t \to \infty$, and the bands of the respective color bands show fits to Eqs. (3). The dark-gray bands show ground-state matrix elements $\mathcal{A}_{0'0}$, and the light-gray bands show the overdetermined fits of these matrix elements to the form factor values $F_{1,2}(Q^2)$.

3 Results

Individual proton and neutron form factors are shown in Fig. 5, similarly compared to phenomenological fits. Although the lattice results have qualitatively similar Q^2 behavior, they overshoot the phenomenological fits by a factor of $(2\ldots2.5)$. This substantial difference may be due to discretization effects. Without a calculation on a smaller lattice spacing, these effects are difficult to assess. A detailed study of $O(a)$-improved current operators and calculations at different lattice spacings are required to control this source of systematic effects.

In Fig. 6, the ratio of proton Pauli and Dirac form factors is shown. In perturbative QCD calculations, this ratio is expected to scale as $F_{2p}/F_{1p} \sim \frac{\log^2(Q^2/\Lambda^2)}{Q^2}$ [17]. The lattice data are compared with the phenomenological fits [16] based on proton experimental data available at $Q^2 \lesssim 8.5\,\text{GeV}^2$ (shown with black symbols). Although the general trend in the data is compatible with the logarithmic growth, the current precision is insufficient to validate it.

The ratios of Sachs electric and magnetic form factors for the proton and the neutron are shown in Figs. 7, and again compared to the phenomenological fits [16] and experimental data, as well as calculations using quark+diquark Faddeev equations [2]. The agreement between lattice data and experiment (phenomenology) for the ratios in the proton case is reassuring, although better precision is certainly required in light of upcoming

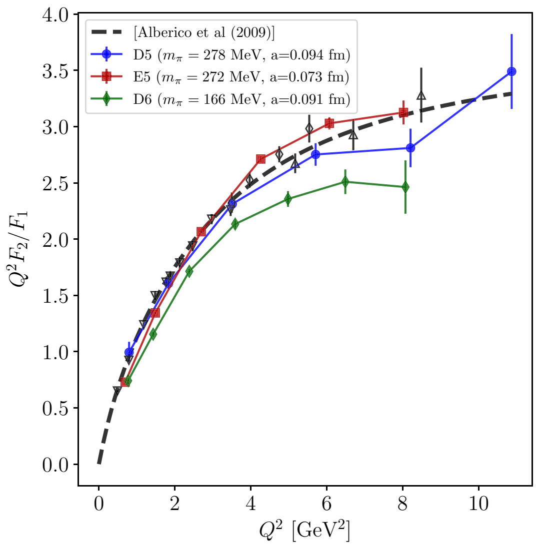

Fig. 6 Ratio of proton Pauli and Dirac form factors $Q^2 F_{2p}(Q^2)/F_{1p}(Q^2)$, compared to phenomenological fits of experimental data [16] (dashed curves). Disconnected quark contractions are neglected

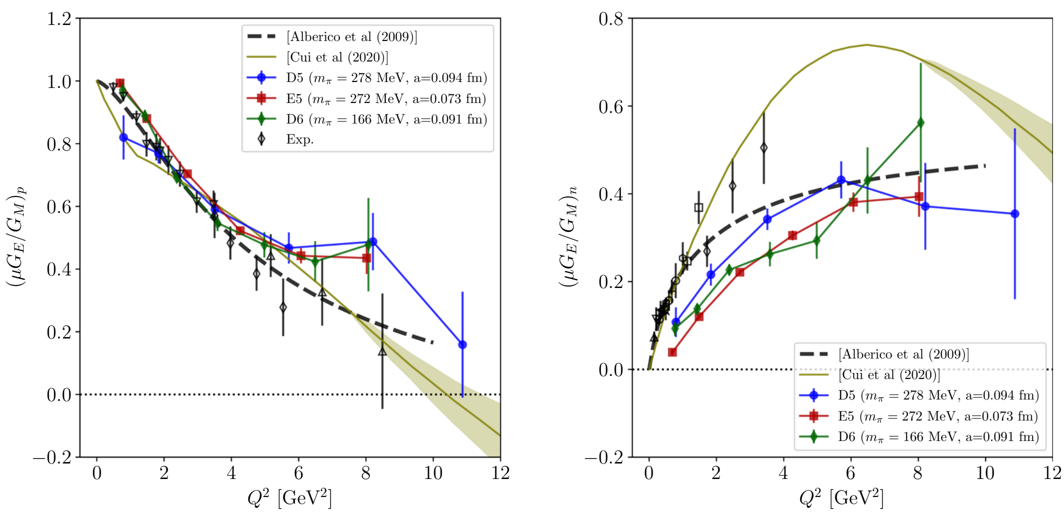

Fig. 7 Ratio of proton (left) and neutron (right) Sachs form factors $\mu G_E/G_M$, compared to phenomenological fits of experimental data [16] and quark+diquark Faddeev equation calculations [2]. Disconnected quark contractions are neglected

new experiments at JLab. In the case of the neutron, the G_{En}/G_{Mn} ratio is below the experimental values, although it demonstrates qualitative agreement in its Q^2 behavior. Since the neutron is neutral, its electric form factor may be much more sensitive to the systematic effects in this calculation, in particular the omission of disconnected quark contractions and unphysical heavy pion masses. We observe, however, that at high momenta where the results should depend less on the masses of the light quarks, the lattice data agrees with extrapolations from phenomenological fits. Better motivated comparisons will be possible with future neutron form factor data with extended Q^2 range.

Finally, in Fig. 8 we show contributions to nucleon form factors from u and d quarks separately. For comparison, these contributions are shown rescaled in the fashion similar to Ref. [18]. In experiment, this can be studied by combining proton and neutron data and relying on $SU(2)_f$ symmetry, which is exact in our lattice QCD calculations. Since both the neutron and the proton data are required, the fit can only be relied upon for $Q^2 \lesssim 3.4\,\mathrm{GeV}^2$. Similarly to the nucleon form factors, lattice results for their flavor consituents overshoot experimental fits by a large factor. Still, it is reassuring that their Q^2 behavior and the relative u and d quark contributions are in qualitative agreement.

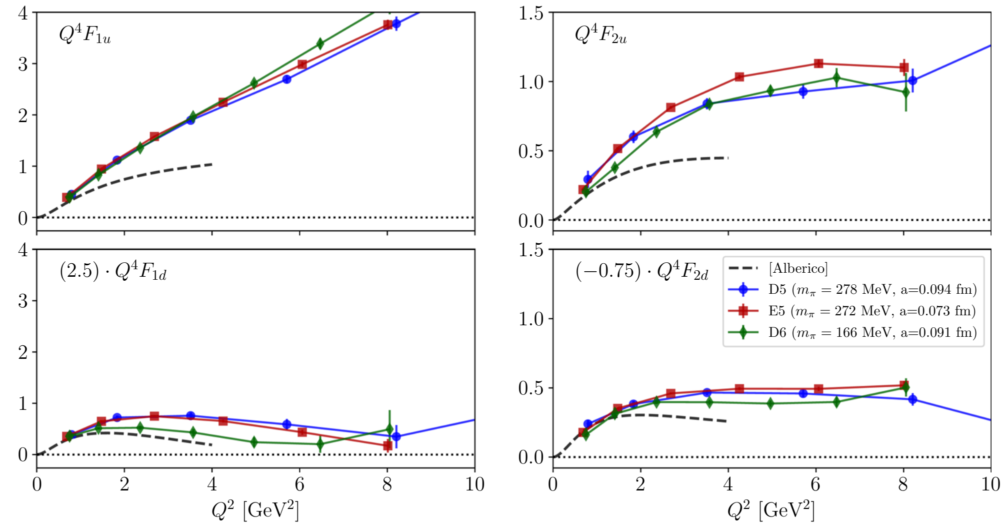

Fig. 8 Contributions of u and d quarks to Dirac F_1 (left) and Pauli F_2 (right) nucleon form factors, scaled by Q^4. The scales are adjusted for comparison to figures in Ref. [18]. Disconnected quark contractions are neglected. The phenomenological fits to experimental data (dashed curves) are limited to $Q^2 \leq 3.4\,\mathrm{GeV}^2$ in the neutron case [16]

4 Conclusions

To summarize, results of these initial lattice QCD calculations of nucleon form factors are overestimating the results of experiment by a large factor. However, the ratios of these form factors are in much better agreement with experiment and phenomenology. Calculations with smaller lattice spacings, which are underway, will lead to better understanding of this disagreement, validate lattice QCD methods for high-momentum nucleon states on a lattice, and shed light on nucleon structure in the important region of transition from nonperturbative to perturbative quark-gluon dynamics.

Acknowledgements S.S. is supported by the National Science Foundation under CAREER Award PHY-1847893. Any opinions, findings, and conclusions or recommendations expressed in this material are those of the author(s) and do not necessarily reflect the views of the National Science Foundation. S.M. is supported by the U.S. DOE, Office of Science, Office of High Energy Physics under Award Number DE-SC0009913. M.E., J.N. and A.P. are supported by the U.S. DOE, Office of Science, Office of Nuclear Physics through grants numbered DE-FG02-96ER40965, DE-SC-0011090 and DE-SC-0023116, respectively. The research reported in this work made use of computing and long-term storage facilities of the USQCD Collaboration, which are funded by the Office of Science of the U.S. Department of Energy. The authors gratefully acknowledge the Gauss Centre for Supercomputing e.V. (www.gauss-centre.eu) for funding this project by providing computing time through the John von Neumann Institute for Computing (NIC) on the GCS Supercomputer JUWELS at Jülich Supercomputing Centre (JSC). This research also used resources of the National Energy Research Scientific Computing Center, a DOE Office of Science User Facility supported by the Office of Science of the U.S. Department of Energy under Contract No. DE-AC02-05CH11231 using NERSC award NP-ERCAP0024043. The computations were performed using the Qlua software suite [19].

Author Contributions Main text and figures prepared by S.S. All authors reviewed the manuscript.

Declarations

Conflict of interest The authors declare no competing interests.

References

1. V. Punjabi, C.F. Perdrisat, M.K. Jones, E.J. Brash, C.E. Carlson, The structure of the nucleon: elastic electromagnetic form factors. Eur. Phys. J. A **51**, 79 (2015). https://doi.org/10.1140/epja/i2015-15079-x. arXiv:1503.01452 [nucl-ex]
2. Z.-F. Cui, C. Chen, D. Binosi, F. Soto, C.D. Roberts, J. Rodríguez-Quintero, S.M. Schmidt, J. Segovia, Nucleon elastic form factors at accessible large spacelike momenta. Phys. Rev. D **102**(1), 014043 (2020). https://doi.org/10.1103/PhysRevD.102.014043. arXiv:2003.11655 [hep-ph]

3. J. Arrington, E. Christy, S. Gilad, B. Moffit, V. Sulkosky, B. Wojtsekhowski, et al.: Precision Measurement of the Proton Elastic Cross Section at High Q^2. Jefferson Lab Experiment 12-07-108, https://www.jlab.org/exp_prog/proposals/07/PR12-07-108.pdf (2007)
4. E. Brash, E. Cisbani, M. Jones, M. Khandaker, N. Liyanage, L. Pentchev, C.F. Perdrisat, V. Punjabi, B. Wojtsekhowski, Large Acceptance Proton Form Factor Ratio Measurements at 13 and 15 $(\text{GeV}/\text{c})^2$ Using Recoil Polarization Method. Jefferson Lab Experiment 12-07-109, https://www.jlab.org/exp_prog/proposals/07/PR12-07-109.pdf (2008)
5. G. Cates, S. Riordan, B. Wojtsekhowski, et al., *Measurement of the Neutron Electromagnetic Form Factor Ratio G_{En}/G_{Mn} at High Q^2*
6. J. Annand, R. Gilman, B. Quinn, B. Wojtsekhowski, et al., *Precision measurement of the Neutron Magnetic Form Factor up to $Q^2 = 18.0(\text{GeV}/c)^2$ by the Ratio Method*. Jefferson Lab Experiment 12-09-019, https://www.jlab.org/exp_prog/proposals/09/PR12-09-019.pdf (2009) (2009) (2009) (2009)
7. W. Brooks, J. Lachniet, M. Vineyard, et al., *Measurement of the Neutron Magnetic Form Factor at High Q^2 Using the Ratio Method on Deuterium*. Jefferson Lab Experiment 12-07-104, https://www.jlab.org/exp_prog/proposals/07/PR12-07-104.pdf (2007)
8. M.E. Christy et al., Form factors and two-photon exchange in high-energy elastic electron-proton scattering. Phys. Rev. Lett. **128**(10), 102002 (2022). https://doi.org/10.1103/PhysRevLett.128.102002. arXiv:2103.01842 [nucl-ex]
9. A.J. Chambers et al., Electromagnetic form factors at large momenta from lattice QCD. Phys. Rev. D **96**(11), 114509 (2017). https://doi.org/10.1103/PhysRevD.96.114509. arXiv:1702.01513 [hep-lat]
10. G.P. Lepage, *The Analysis of Algorithms for Lattice Field Theory*. Invited lectures given at TASI'89 Summer School, Boulder, CO, 4–30 June 1989
11. S. Syritsyn, A.S. Gambhir, B. Musch, K. Orginos, *Constructing Nucleon Operators on a Lattice for Form Factors with High Momentum Transfer*. PoS LATTICE2016, 176 (2017)
12. C. Kallidonis, S. Syritsyn, M. Engelhardt, J. Green, S. Meinel, J. Negele, A. Pochinsky, Nucleon electromagnetic form factors at high Q^2 from Wilson-clover fermions. in *36th International Symposium on Lattice Field Theory (Lattice 2018) East Lansing*, MI, United States, 22-28 July 2018 (2018)
13. G.S. Bali, B. Lang, B.U. Musch, A. Schäfer, Novel quark smearing for hadrons with high momenta in lattice QCD. Phys. Rev. D **93**(9), 094515 (2016). https://doi.org/10.1103/PhysRevD.93.094515. arXiv:1602.05525 [hep-lat]
14. S.N. Syritsyn, J.D. Bratt, M.F. Lin, H.B. Meyer, J.W. Negele et al., Nucleon electromagnetic form factors from lattice QCD using 2+1 flavor domain wall fermions on fine lattices and chiral perturbation theory. Phys. Rev. D **81**, 034507 (2010). https://doi.org/10.1103/PhysRevD.81.034507. arXiv:0907.4194 [hep-lat]
15. J. Green, S. Meinel, M. Engelhardt, S. Krieg, J. Laeuchli, J. Negele, K. Orginos, A. Pochinsky, S. Syritsyn, High-precision calculation of the strange nucleon electromagnetic form factors. Phys. Rev. D **92**, 031501 (2015). https://doi.org/10.1103/PhysRevD.92.031501. arXiv:1505.01803 [hep-lat].[Phys. Rev.D92,031501(2015)]
16. W.M. Alberico, S.M. Bilenky, C. Giunti, K.M. Graczyk, Electromagnetic form factors of the nucleon: new Fit and analysis of uncertainties. Phys. Rev. C **79**, 065204 (2009). https://doi.org/10.1103/PhysRevC.79.065204. arXiv:0812.3539 [hep-ph]
17. A.V. Belitsky, X.-D. Ji, F. Yuan, A perturbative QCD analysis of the nucleon's Pauli form-factor $F_2(Q^2)$. Phys. Rev. Lett. **91**, 092003 (2003). https://doi.org/10.1103/PhysRevLett.91.092003. arXiv:hep-ph/0212351 [hep-ph]
18. G.D. Cates, C.W. Jager, S. Riordan, B. Wojtsekhowski, Flavor decomposition of the elastic nucleon electromagnetic form factors. Phys. Rev. Lett. **106**, 252003 (2011). https://doi.org/10.1103/PhysRevLett.106.252003. arXiv:1103.1808 [nucl-ex]
19. A. Pochinsky, *Qlua Lattice Software Suite*. https://usqcd.lns.mit.edu/qlua (2008–present)